

## Singlemode versus multimode calculations of Raman intensities of cytochrome c

P. M. Champion and A. C. Albrecht

Citation: *The Journal of Chemical Physics* **75**, 3211 (1981); doi: 10.1063/1.442493

View online: <http://dx.doi.org/10.1063/1.442493>

View Table of Contents: <http://scitation.aip.org/content/aip/journal/jcp/75/7?ver=pdfcov>

Published by the [AIP Publishing](#)

---

### Articles you may be interested in

[Single-mode tapered waveguide laser in Er-doped glass with multimode-diode pumping](#)

*Appl. Phys. Lett.* **82**, 1332 (2003); 10.1063/1.1557771

[Singlemode and multimode Rayleigh–Taylor experiments on Nova](#)

*Phys. Plasmas* **2**, 241 (1995); 10.1063/1.871096

[Comparison of multimode and singlemode optical fibers for quasielastic light scattering](#)

*Rev. Sci. Instrum.* **61**, 2001 (1990); 10.1063/1.1141414

[Generation of high intensity cw stimulated Raman scattering in a singlemode fiber](#)

*J. Appl. Phys.* **63**, 2882 (1988); 10.1063/1.340948

[Singlemode or controlled multimode microwave cavity applicators for precision materials processing](#)

*Rev. Sci. Instrum.* **58**, 1477 (1987); 10.1063/1.1139384

---



# Single-mode versus multimode calculations of Raman intensities of cytochrome *c*

P. M. Champion and A. C. Albrecht

*Laboratory of Atomic and Solid State Physics and Department of Chemistry, Cornell University, Ithaca, New York 14853*

(Received 30 March 1981; accepted 22 June 1981)

The simple single-mode model for Raman scattering is examined with regard to the relative Raman intensity ratios of cytochrome *c* at the 0-0 and 0-1 transition frequencies of  $S_1$  and  $S_2$ . Interference between *A*- and *B*-term amplitudes as well as nonadiabatic effects are considered. The model is found to generate the experimentally observed intensity ratios only under the condition that the damping factors in  $S_2$  (Soret band) and  $S_1$  (Q band) are nearly equal. This condition is at variance with observation unless multimode effects are included to account for the large bandwidth of  $S_2$  in cytochrome *c*. Use of the multimode model generates the observed Raman intensity ratios in  $S_2$  without the need for *A*- and *B*-term interference effects.

The study of resonance Raman scattering intensity as a function of laser excitation wavelength (i.e., the Raman excitation profile, REP) can be a useful tool for the understanding of excited molecular states. A variety of phenomena can contribute to the overall resonance scattering amplitudes of a given Raman active vibrational mode. Within the adiabatic approximation two main sources of scattering amplitude are normally identified: the *A* term (Franck-Condon activity) and the *B* term (intermanifold vibronic activity).<sup>1</sup> Strictly speaking these sources must be considered in the full  $3N-6$  vibrational subspace of the molecule. In fact, the shape of the REP of a given vibration may be dominated by other vibrations that are strongly coupled to the transition; and, furthermore, even when modes are weakly coupled to the electronic transition, if their number is sufficiently large, they will have a conspicuous influence on the shape of the REP.<sup>2,3</sup> Nonadiabatic corrections, though generally small, can also lead to detectable effects in the structure of the REP.<sup>4</sup>

If one ignores the multimode vibrational subspace and derives the REP from a single-mode *A*-term point of view, a very simple profile is obtained (particularly in the limit of weak Franck-Condon coupling, i.e., small potential well shifts). In this limit the only important Raman Franck-Condon factors involved in *A*-term scattering are  $\langle 0|0\rangle\langle 0|1\rangle$  (at the zero-zero transition frequency) and  $\langle 0|1\rangle\langle 1|1\rangle \approx -\langle 0|0\rangle\langle 0|1\rangle$  (at the zero-one transition frequency). Thus, the single mode *A*-term amplitudes are equal in magnitude but opposite in phase. The REP then shows two peaks of equal intensity: one at the 0-0 frequency and the other at the 0-1 frequency of the electronic transition. However, if some *B*-term activity is also present, even within the single mode picture, interesting asymmetric interferences can occur due to the fact that the *B*-term scattering amplitudes have the same phase at both the 0-0 and 0-1 frequencies.

Recently a careful experimental study was made of the REP of the  $1362\text{ cm}^{-1}$  ( $a_{1g}$ ) mode in the Soret band ( $S_2$ ) of ferrocytochrome *c*. The profile proves to be quite asymmetric.<sup>2</sup> Its shape is successfully rationalized in terms of an *A*-term model but within a multimode context.<sup>2,3</sup> On the other hand, calculations based on simple (single-mode) *A*- and *B*-term interferences have been

applied to the REP's observed in metalloporphyrins and ferrocytochrome *c*.<sup>5,6</sup> In particular, Shelnutt<sup>6</sup> found that this model can generate a good qualitative fit to the shape of the asymmetric REP of the  $1362\text{ cm}^{-1}$  vibration by using *B*-term interference from the vibronically coupled Q state ( $S_1$ ) to alter the single mode *A* term of the Soret band ( $S_2$ ). Large homogeneous bandwidths ( $900\text{ cm}^{-1}$  FWHM) were required to "fill out" the profile in the Soret band (this is inevitable for all single-mode models). Similarly, rather large homogeneous bandwidths ( $400\text{ cm}^{-1}$  FWHM) were used in the Q band region in order to minimize the differences between the observed and calculated Raman intensities for resonance with  $S_1$  and  $S_2$ . Most significantly, it was found that this simple single-mode  $S_1/S_2$  interference model failed on quantitative grounds and the predicted intensity ratio of the  $S_2$  REP to the  $S_1$  REP fell short of the observed ratio by a factor of 4, even when using the excessive  $400\text{ cm}^{-1}$  bandwidth for  $S_1$  (the maximum possible  $S_1$  bandwidth is approximately  $150\text{ cm}^{-1}$  and there is reason to believe that it is somewhat smaller, see Ref. 7).

In the multimode *A*-term model<sup>2,3</sup> both the asymmetric shape of the Soret REP and the intensity were fit, since that model is not constrained by parameters derived from the Q band (i.e., the REP in  $S_2$  is dominated by multimode *A*-term effects and can thus be scaled independently of the *B*-term coupling with  $S_1$ ). Given the quantitative failure of the single-mode  $S_1/S_2$  interference model, Shelnutt suggested that additional *B*-term sources from higher lying electronic states (e.g.,  $S_3$ ) may be active. The multimode model was criticized for requiring homogeneous bandwidths for  $S_2$  which are smaller than those claimed for  $S_1$  (see Ref. 7, however). The multimode model was therefore not considered as a serious alternative. As a matter of fact, in the multimode model, the homogeneous bandwidth is a "soft" parameter and can vary considerably without significantly altering the absorption bandwidth or the REP shape.<sup>2,3</sup>

In the present communication we show how additional *B*-term sources from higher lying electronic states are absent and that the modeling of the Soret REP must succeed within the  $S_1/S_2$  system of electronic states. We see how the elaborate computer calculations for test-

ing the single-mode  $S_1/S_2$  interference model<sup>6</sup> can be mimicked by simple algebraic statements which reveal the limits of this model and how it must fail at the quantitative level. We conclude that the multimode *A*-term model appears to capture the essence of the Soret REP of the 1362  $\text{cm}^{-1}$  mode. Generally speaking, as resonance with a strongly allowed electronic transition is approached, one expects the *A*-term to overcome the *B*-term sources of scattering.<sup>1</sup> It appears that the Soret band of cytochrome *c* is no exception.

A search for *B*-term sources of scattering at energies above the Soret state in the cytochrome *c* system was made at three separate wavelengths: at 337 nm,<sup>2</sup> and more recently at 317 and 257 nm.<sup>8</sup> At neither of the latter two wavelengths was Raman scattering from the heme group detected. In particular we note that the absorption spectrum of ferrocyanochrome *c* shows a feature at about 315 nm [ $\epsilon_{315} = 36 \text{ (mM-cm)}^{-1}$ ] which is comparable to the intensity of the *Q* band ( $S_1$ ). In order to check more carefully for possible contributions from this "state," comparative studies were carried out on identical samples of ferrocyanochrome *c* (23  $\mu\text{M}$  concentration, 1.5 o.d. at Soret maximum in 5 mm cuvette) using visible and near ultraviolet excitation. Raman scattering in the  $S_1$  region is easily observed under these conditions and the 1362  $\text{cm}^{-1}$  band can be compared directly to the 1 M  $\text{SO}_4^{2-}$  internal standard. At 514.5 nm excitation [ $\epsilon_{515} = 12.6 \text{ (mM-cm)}^{-1}$ ] we find that the ratio of the peak height of the 1362  $\text{cm}^{-1}$  band to the standard band is approximately 0.08. This agrees well with the experimental relative intensities presented previously by Shelnutt.<sup>6</sup> On the other hand, a sample of 23  $\mu\text{M}$  ferrocyanochrome excited at 317 [ $\epsilon_{317} = 32 \text{ (mM-cm)}^{-1}$ ] shows no trace of Raman scattering from the heme chromophore. Only the internal standard band of sulfate is observed with a signal to (rms) noise level of approximately 70/1. We therefore conclude that no significant (*A*- or *B*-term) source of scattering from the state at 315 nm is present which is comparable to the scattering seen in  $S_1$ . Thus, since the feature at 315 nm and the Soret band are of comparable widths, the Soret band REP must be rationalized within the  $S_1/S_2$  system of electronic states without recourse to coupling with electronic states to the blue of the Soret band.

Next we delineate the constraints of the single mode  $S_1/S_2$  interference model<sup>6</sup> by presenting an algebraic analysis based on simple stick scattering amplitudes. Since  $a_{1g}$  modes do not couple the nearly degenerate  $x$ - $y$  states associated with the heme group, it is sufficient to treat the  $x$ -polarized states of  $S_1$  and  $S_2$  independently of the  $y$ -polarized states (note that each set will lead to essentially the same REP). Thus, the two state model can describe the resonance behavior of  $a_{1g}$  modes as long as additional electronic states do not contribute significantly to the scattering amplitudes and the  $x, y$  splitting in  $S_1$  and  $S_2$  is small compared to the Raman active quantum (as observed in  $S_1$ ).

For resonance with a single electronic state,  $|e\rangle$ , vibronically coupled to one additional state,  $|s\rangle$ , the *A*- and *B*-term amplitudes for the Raman transition can be written in the following explicit forms<sup>1,4</sup>:

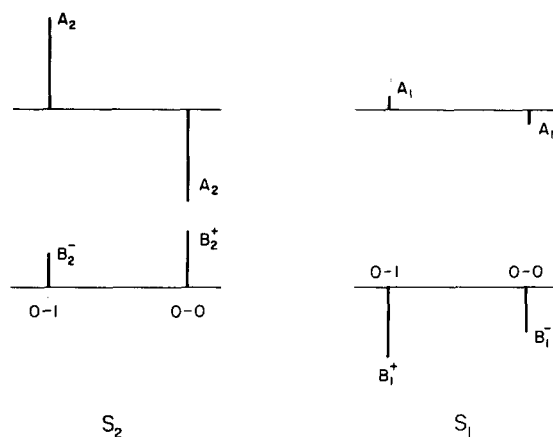


FIG. 1. The *A*- and *B*-term amplitudes for exact resonance with the 0-0 and 0-1 transitions of  $S_1$  and  $S_2$  are given. Explicit expressions for the various amplitudes can be found in Eq. (2) of the text. The phases of the amplitudes are given by the upward (+) or downward (-) direction of the stick amplitudes. The relative phasing between the *A* and *B* amplitudes is, *a priori*, unknown for  $a_{1g}$  modes. In this example we have chosen the phases so that the Raman intensity at the 0-1 transition of  $S_2$  will be maximally enhanced. The zero-point energy separation between  $S_1$  and  $S_2$  is denoted by  $|\Delta|$  in the text and corresponds to the separation between the two 0-0 transitions; the magnitude of  $\Delta$  is 5800  $\text{cm}^{-1}$  for ferrocyanochrome *c*. The energy separation between the 0-0 and 0-1 transitions corresponds to the Raman active quantum  $\hbar\omega$  and is 1362  $\text{cm}^{-1}$  for this analysis.

$$A = \sum_v \frac{\langle g|R|e\rangle\langle e|R|g\rangle\langle 0|v\rangle\langle v|1\rangle}{E_v - \hbar\nu_L - i\Gamma_e},$$

$$B = \sum_v \frac{\langle g|R|e\rangle\langle s|R|g\rangle\langle e|dV/dQ|s\rangle\langle 0|v\rangle\langle v|Q|1\rangle}{(E_v - \hbar\nu_L - i\Gamma_e)(\Delta - \hbar\omega)} + \frac{\langle g|R|s\rangle\langle e|R|g\rangle\langle s|dV/dQ|e\rangle\langle 0|Q|v\rangle\langle v|1\rangle}{(E_v - \hbar\nu_L - i\Gamma_e)(\Delta + \hbar\omega)}, \quad (1)$$

where  $Q$  is the normal coordinate of the Raman active mode and  $v$  represents the occupation number of the excited vibrational state of  $|e\rangle$ . The transition dipole matrix elements are given by  $\langle g|R|e\rangle$  and  $\langle g|R|s\rangle$ , while  $\langle e|dV/dQ|s\rangle$  represents the vibronic coupling responsible for mixing the two crude adiabatic states  $|e\rangle$  and  $|s\rangle$ . For simplicity, the damping factor  $\Gamma_e$  is taken to be independent of  $v$  (see Ref. 9).  $E_v$  is the electronic plus vibrational energy of the resonant state and  $\hbar\nu_L$  is the incident photon energy. The quantity  $\Delta$  represents the zero-point energy separation of states  $|e\rangle$  and  $|s\rangle$  (i.e.,  $\Delta = E_e^0 - E_s^0$ ) while  $\hbar\omega$  is the energy of the Raman active vibration. This latter vibrational correction to the electronic energy gap between  $|e\rangle$  and  $|s\rangle$  represents the leading "nonadiabatic" correction to the REP.<sup>4</sup>

To elucidate the model we display in Fig. 1, hypothetical relative magnitudes and phases of the *A*- and *B*-term contributions to the scattering amplitudes for resonance with both the  $S_2$  (Soret) and  $S_1$  (*Q* band) transitions. The amplitudes in exact resonance with the 0-0 and 0-1 transitions of each state are shown as sticks pointing upward or downward to represent, respectively, the positive or negative phase factors. In order to approximate the observed asymmetry of the REP in  $S_2$ ,<sup>2</sup> the phase be-

tween the *A*- and *B*-term amplitudes has been chosen to maximally enhance the 0–1 scattering in the Soret region.<sup>6</sup> The nonadiabatic corrections to the *B*-term amplitudes have also been included. To be more specific, we use Eq. (1) to find single mode, single state resonance expressions ( $\hbar\nu_L = E_v$ ) for the *A*- and *B*-term amplitudes for  $S_1$  scattering ( $|e\rangle = S_1$ ,  $|s\rangle = S_2$ ) and for  $S_2$  scattering ( $|e\rangle = S_2$ ,  $|s\rangle = S_1$ ):

$$A_1 = M_{A1}[S_1]^2/\Gamma_1, \quad (2a)$$

$$A_2 = M_{A2}[S_2]^2/\Gamma_2, \quad (2b)$$

$$B_1^* = M_B^*[S_1][S_2]/\Gamma_1, \quad (2c)$$

$$B_2^* = M_B^*[S_1][S_2]/\Gamma_2, \quad (2d)$$

where the subscripts 1 and 2 label the first and second excited singlet states. The quantities  $[S_1]$  and  $[S_2]$  represent the electronic transition dipole matrix elements, while  $\Gamma_1$  and  $\Gamma_2$  are the damping factors associated with the two electronic states. The remaining terms labeled *M* represent Raman Franck–Condon factors for the *A*-terms and nonadiabatic vibronic coupling strengths for the *B*-terms [see Eq. (1)].

We now proceed to find a set of relationships between the *A*- and *B*-term amplitudes and the damping factors ( $\Gamma_1$  and  $\Gamma_2$ ) that must be satisfied in order for this single-mode model to be consistent with the experimentally observed resonance Raman intensities.<sup>2,6</sup> To begin with, we can use Fig. 1 as a guide to calculate the theoretical Raman intensity ratios. Squaring the summed amplitudes gives the ratio of the Raman intensities at the 0–1 and 0–0 transition frequencies of  $S_2$ :

$$R_{10}^{(2)} = I_{01}^{S_2}/I_{00}^{S_2} = (A_2 + B_2^*)^2/(B_2^* - A_2)^2. \quad (3)$$

Similarly, the ratio of the Raman intensities at the 0–1 and 0–0 transitions of  $S_1$  is given by

$$R_{10}^{(1)} = I_{01}^{S_1}/I_{00}^{S_1} = (A_1 - B_1^*)^2/(A_1 + B_1^*)^2 \quad (4)$$

and, finally, the ratio of the Raman intensity at the 0–1 transition of  $S_2$  to the intensity of the 0–0 transition of  $S_1$  is given by

$$R_{10}^{(2,1)} = I_{01}^{S_2}/I_{00}^{S_1} = (A_2 + B_2^*)^2/(A_1 + B_1^*)^2. \quad (5)$$

If we now define the parameters:

$$\Theta = A_2/B_2^*, \quad (6a)$$

$$\Phi = B_1^*/A_1, \quad (6b)$$

$$\gamma = \Gamma_2/\Gamma_1, \quad (6c)$$

we can use Eq. (2) to rewrite Eqs. (3)–(5) in the following manner:

$$R_{10}^{(2)} = (\Theta + 1)^2/(\mu - \Theta)^2, \quad (7a)$$

$$R_{10}^{(1)} = (1 - \mu\Phi)^2/(1 + \Phi)^2, \quad (7b)$$

$$R_{10}^{(2,1)} = (\Phi\Theta + \Phi)^2/(\gamma + \gamma\Phi)^2, \quad (7c)$$

where  $\mu$  is the ratio  $M_B^*/M_B^- = (|\Delta| + \hbar\omega)/(|\Delta| - \hbar\omega)$ . For the present application  $|\Delta| = 5800 \text{ cm}^{-1}$  and  $\hbar\omega = 1362 \text{ cm}^{-1}$ , so that  $\mu = 1.6$ . Using the experimentally determined values for the three ratios<sup>2,6</sup> we have  $R_{10}^{(1)} \approx 2$ ,  $R_{10}^{(2)} \approx 2$ , and  $R_{10}^{(2,1)} \approx 48$  (see Ref. 10) which leads to a unique solution for the unknowns

$$\Theta = 7.9, \quad (8a)$$

$$\Phi = 13.0, \quad (8b)$$

$$\gamma = 1.2. \quad (8c)$$

Equation (8c) is especially interesting since an upper limit of  $50 \text{ cm}^{-1}$  for  $\Gamma_1$  ( $100 \text{ cm}^{-1}$  FWHM) can be deduced from the width of the  $S_1$  absorption band of ferrocycytochrome *c*.<sup>7</sup> Thus, a maximum value for  $\Gamma_2$  is found to be  $60 \text{ cm}^{-1}$  ( $120 \text{ cm}^{-1}$  FWHM). The fundamental contradiction that arises is that the observed fullwidth of the Soret band ( $S_2$ ) approaches  $1300 \text{ cm}^{-1}$ , an order of magnitude larger than the maximum FWHM allowed within this single-mode model!

How, then, do we account for the large absorption bandwidth of  $S_2$  if we limit ourselves to a single-mode model? If we take the extreme view that the Soret band is predominantly homogeneously broadened with  $\Gamma_2 \approx 500 \text{ cm}^{-1}$  ( $1000 \text{ cm}^{-1}$  FWHM), we find  $\gamma \approx 10$  and, using Eq. (7c), we have  $R_{10}^{(2,1)} \approx 0.75$  not the observed 48. In the previous analysis,<sup>6</sup> an attempt was made to resolve the problem by using an intermediate value for  $\gamma$  ( $900 \text{ cm}^{-1}/400 \text{ cm}^{-1} = 2.25$ ). This choice of  $\gamma$  still predicts significantly larger relative scattering intensities in the  $Q$ -band region than are observed<sup>10</sup> [i.e.,  $R_{10}^{(2,1)} = I_{01}^{S_2}/I_{00}^{S_1} = 12$  (Ref. 6) vs  $R_{10}^{(2,1)} = 48$  (experimental)]. This discrepancy can be deduced directly from Eq. (7c) where it can be seen that a change in  $\gamma$  by a factor of 2 (1.2 vs 2.25) results in a decrease of  $R_{10}^{(2,1)}$  by a factor of 4. Clearly, the single-mode (*A*- and *B*-term interference) model fails to account simultaneously for the observed relative Raman intensities and the absorption bandwidths of ferrocycytochrome *c*.

As we have remarked, a straightforward resolution of this dilemma results if we consider the effect of the full multimode subspace of  $a_{1g}$  vibrations which, in any case, is observed to be resonantly Raman active upon Soret band excitation.<sup>2</sup> If this subspace is incorporated into the calculation, the  $I_{01}^{S_2}/I_{00}^{S_2}$  ratio increases without the necessity of *B*-term interference. In addition to fitting the Soret band REP, this model explains the general shape of the Soret absorption band.<sup>2,3</sup> Inclusion of the multimode approach in the present analysis relaxes the restriction of Eq. (3) and allows  $\Theta = A_2/B_2^*$  to take on values greater than 7.9 (i.e., the multimode *A* term alone generates the ratio  $R_{10}^{(2)}$  and interference with the *B* term is no longer necessary to explain the data). This in turn [see Eq. (7c)] may lead to an increase of  $\gamma$  from the single-mode value of 1.2 (approximate upper limits on  $\Gamma_1$  and  $\Gamma_2$  are discussed in Refs. 2, 3, and 7). In any case, the entire single-mode analysis suffers a serious breakdown once the multimode effects are acknowledged, since the original choice of phasing in Fig. 1 (and Ref. 6) is no longer required.

In conclusion, it is our view that in the Soret band of ferrocycytochrome *c* the dominant scattering mechanism is, indeed, the multimode *A* term.<sup>2,3,11</sup> This view should be contrasted with the single-mode model which invokes significant *A*- and *B*-term interference effects to explain the REP but does not simultaneously account for the absorption bandwidths.<sup>6</sup> Some weak interference effects in  $S_2$  from *B*-term coupling are possible, in our opinion,

and further experiments are needed in order to determine with accuracy the magnitude of this effect. In the Q band region, on the other hand, the theoretical analysis of resonance scattering is severely complicated by the significant interference between A- and B-term scattering mechanisms (with undetermined phase) as well as by the unusual polarization behavior.<sup>10</sup>

This work was partially supported by the Materials Science Center of Cornell University and by a grant from the National Institutes of Health AM20379. One of us (ACA) thanks the National Science foundation for support under grant CHE-8016526.

<sup>1</sup>J. Tang and A. C. Albrecht, in *Raman Spectroscopy*, edited by H. Szymanski (Plenum, New York, 1970); A. C. Albrecht and M. C. Hutley, *J. Chem. Phys.* 55, 4438 (1971).

<sup>2</sup>P. M. Champion and A. C. Albrecht, *J. Chem. Phys.* 71, 1110 (1979).

<sup>3</sup>P. M. Champion and A. C. Albrecht, *J. Chem. Phys.* 72, 6498 (1980).

<sup>4</sup>G. J. Small and E. S. Yeung, *Chem. Phys.* 9, 379 (1975).

<sup>5</sup>M. Zgierski, J. A. Shelnutt, and M. Pawlikowski, *Chem. Phys. Lett.* 68, 262 (1979).

<sup>6</sup>J. A. Shelnutt, *J. Chem. Phys.* 72, 3948 (1980); see also *J. Chem. Phys.* 74, 6644 (1981), where a multi mode point of view is included. However, the perturbation approach used there invokes ground state vibrational wave functions as a basis set and must diverge exponentially in coupling strength/number of CF active vibrations. It therefore is limited to cases in which there are only a small number of weakly coupled vibrations, and cannot incorporate the more extensive multimode model we regard as valid for the cytochrome *c* problem.

<sup>7</sup>The actual value for the FWHM of  $S_1$  is probably somewhat less than 100 cm<sup>-1</sup>; see P. M. Champion and R. Lange, *J. Chem. Phys.* 73, 5947 (1980); P. M. Champion and G. J. Perreault, *J. Chem. Phys.* 75, 490 (1981).

<sup>8</sup>B. Stallard (unpublished results).

<sup>9</sup>The assumption that the damping factor,  $\Gamma_e$ , is independent of the vibrational state is made in order to facilitate the comparison between the single-mode (Ref. 6) and multimode (Ref. 2) models, both of which employ this approximation. It is interesting to note, however, that if we assign different damp-

ing factors to the 0-0 and 0-1 transitions of  $S_2$  (i.e.,  $\Gamma_{20}$  and  $\Gamma_{21}$ ) and consider only single-mode A-term scattering, we have [from Eqs. (2) and (3)]  $R_{10}^{(2)} = \Gamma_{20}/\Gamma_{21} \approx 2$  (experimental). This, however, would imply that the lifetime of the zero-point state of  $S_2$  is two times shorter than the vibrationally excited state of  $S_2$ . This is quite an unusual result and so, for the present, we prefer the simplifying approximation  $\Gamma_{e\nu} = \text{const.}$

<sup>10</sup>We have used the experimentally observed value for  $R_{10}^{(2,1)} \approx 48$  taken from Ref. 6 in which the single-mode model for explaining the REP of  $S_2$  is put forth. In fact the 1362 cm<sup>-1</sup> Raman line shows anomalous polarization when excited in the region between the 0-0 and 0-1 transitions of  $S_1$  [see D. W. Collins, D. B. Fitchen, and A. Lewis, *J. Chem. Phys.* 59, 5714 (1973)]. This polarization behavior is not accounted for within the single-mode model as treated either here or in Ref. 6. In fact, the anomalous polarization behavior in  $S_1$  may be due either to accidental degeneracy of Raman modes of different symmetry or to the lowering of the  $D_{4h}$  point group of the heme system. In the latter case the polarizability tensor for totally symmetric modes could contain an antisymmetric component. In the case of accidental degeneracy, the value of  $R_{10}^{(2,1)}$  relevant to the single-mode model under discussion must have a lower bound of 48. If, on the other hand, the anomalous polarization has its origins in breakdown of symmetry, the REP in the  $S_1$  region must be modeled to include antisymmetric scattering. In any case the extent of anomalous scattering at the 0-0 and 0-1 transitions of  $S_1$  (the points of reference taken here) is greatly reduced from that seen midway between these bands (see Collins *et al.*). Furthermore, for  $S_2$  excitation, no anomalous polarization is encountered. The dominant role of simple, symmetric, A-term scattering in the  $S_2$  REP seems to successfully mask antisymmetric contributions to the polarizability tensor, whatever their origins. The argument presented here will show how the single-mode model is unable to rationalize, consistently, the bandwidth and the REP of  $S_2$ . Logic dictates that we employ parameters in our argument which favor the single-mode model. It is only for this reason that what may really be a lower limit of  $R_{10}^{(2,1)}$  is accepted as its correct value, just as we have taken the phasing of the A and B amplitudes (Fig. 1) to be optimal for the single-mode model.

<sup>11</sup>We note that Soret band preresonance profiles of analogous  $a_1g$  modes in other heme systems are fit quite well using only the A-term contribution; see T. C. Strekas, J. A. Packer, and T. G. Spiro, *J. Raman Spectrosc.* 1, 197 (1973).